Research Article J. Electrochem. Sci. Technol., 2021, 12(1), 67-73

Triphenyl phosphate as an Efficient Electrolyte Additive for Ni-rich NCM Cathode Materials

Kwangeun Jung[1,2], Si Hyoung Oh[3]*, and Taeeun Yim[1,2]*

[1]*Department of Chemistry, Incheon National University, 119 Academy-ro, Yeonsu-gu, Incheon 22012, Republic of Korea*
[2]*Research Institute of Basic Sciences, College of Natural Science, Incheon National University, 119 Academy-ro, Yeonsu-gu, Incheon 22012, Republic of Korea*
[3]*Center for Energy Storage Research, Korea Institute of Science and Technology, 5, Hwarang-ro 14-gil, Seongbuk-gu, Seoul, 02792, Republic of Korea*

ABSTRACT

Nickel-rich lithium nickel-cobalt-manganese oxides (NCM) are viewed as promising cathode materials for lithium-ion batteries (LIBs); however, their poor cycling performance at high temperature is a critical hurdle preventing expansion of their applications. We propose the use of a functional electrolyte additive, triphenyl phosphate (TPPa), which can form an effective cathode-electrolyte interphase (CEI) layer on the surface of Ni-rich NCM cathode material by electrochemical reactions. Linear sweep voltammetry confirms that the TPPa additive is electrochemically oxidized at around 4.83 V (vs. Li/Li^+) and it participates in the formation of a CEI layer on the surface of NCM811 cathode material. During high temperature cycling, TPPa greatly improves the cycling performance of NCM811 cathode material, as a cell cycled with TPPa-containing electrolyte exhibits a retention (133.7 mA h g^{-1}) of 63.5%, while a cell cycled with standard electrolyte shows poor cycling retention (51.3%, 108.3 mA h g^{-1}). Further systematic analyses on recovered NCM811 cathodes demonstrate the effectiveness of the TPPa-based CEI layer in the cell, as electrolyte decomposition is suppressed in the cell cycled with TPPa-containing electrolyte. This confirms that TPPa is effective at increasing the surface stability of NCM811 cathode material because the TPPa-initiated PO_x-based CEI layer prevents electrolyte decomposition in the cell even at high temperatures.

Keywords : Lithium Ion Battery, Nickel-Rich Cathode, Additive, Phosphate, Cathode-Electrolyte Interphases

Received : 16 March 2020, Accepted : 20 August 2020

1. Introduction

In the early 2010s, layered lithium nickel-cobalt-manganese oxides (NCMs) were viewed as prominent cathode materials for new lithium-ion battery (LIB) applications, such as electric vehicles and advanced transportation [1-5]. These applications require a substantially improved energy density of LIBs compared to small-scale devices, so exploration for advanced electrode materials has become a very significant task in the LIB industry to satisfy the specifications of large-scale applications. In this regard, NCMs are considered as good candidates for improving the overall energy density of LIBs because the specific capacity of NCM cathode material can be easily tunable by controlling the Ni composition in the layered NCM cathode material [6-8].

The electrochemical potential of $Ni^{2+} \leftrightarrow Ni^{4+}$ is lower than that of $Co^{3+} \leftrightarrow Co^{4+}$; therefore, increasing the Ni composition in the layered structure of an NCM cathode material allows greater utilization of the specific capacity of the NCM cathode material, thereby improving the energy density of LIBs [9-12]. Many attempts have been made to develop Ni-rich NCM cathode materials, such as NCM622 [13-15], NCM721, NCM712 [16-20], and NCM811, to increase the specific capacity of the cell [21-25]. However, despite their obvious advantages, NCM materials still suffer from poor cycling performance, especially at high temperature. In general, the spe-

*E-mail address: yte0102@inu.ac.kr and sho74@kist.re.kr

DOI: https://doi.org/10.33961/jecst.2020.00850

cific capacity of NCM cathode material increases as its Ni content increases in the layered structure, but unstable Ni^{4+} (the electrochemical charging product) triggers electrolyte decomposition at the interfaces between the NCM cathode and the electrolyte, leading to rapid fading of the cell [26-30].

This electrolyte decomposition is much more severe at high temperature, implying a significant vulnerability of NCM cathode material is to high temperatures when compared with other conventional cathode materials. To overcome these problems, many strategies have been intensively explored, including: 1) development of NCM cathode material coated with oxides such as Al_2O_3, SiO_2, and ZrO_2 [31-35], 2) modification of NCM surface by the introduction of artificial cathode-electrolyte interphases (CEI) [36-40], and 3) use of functional additives in the electrolytes that can form a CEI layer on the surface of the NCM cathode material [41-45]. In recent studies, it has been reported that functional electrolyte additives evidently improve electrochemical performances of the Ni-rich NCM cathode material such as TPPO [46], DODSi [47], SA [48], 2-TS [49], and BFS [50], which have task-specific functional groups on the molecular structure of electrolyte additives. In other word, use of electrolyte additive can be considered as one of efficient method to improve electrochemical performance of the NCM cathode materials.

In this study, we propose a functional electrolyte additive, triphenyl phosphate (TPPa), which can form an effective CEI layer on the surface of Ni-rich NCM cathode material by an electrochemical reaction (Fig. 1). The electrochemical oxidation of the TPPa additive is anticipated to form a phosphate (PO_x)-based CEI layer after several initial cycles, and this layer will effectively decrease electrolyte decomposition in the cell. According to the published literature, the localized charge in the PO_x functional group allows selective ion migration by an ion-hopping mechanism [51-55]. In addition, the PO_x-based CEI layer effectively stabilizes the interface of typical cathode materials because it efficiently protects the cathode material from undesired electrochemical/chemical reactions during the charging/discharging processes [56-58]. This means that once the PO_x-based CEI layer is formed by the electrochemical reaction of TPPa, it can improve the electrochemical performance of the cell by acting as an ionic conductor and

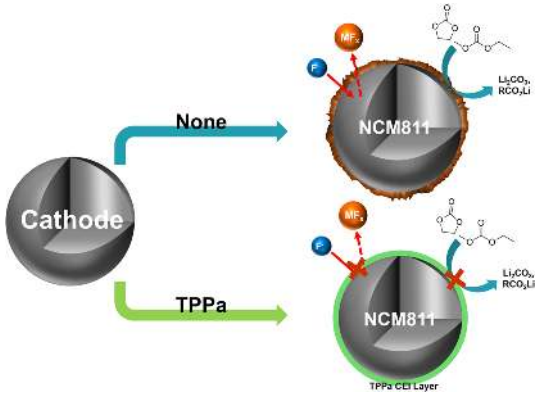

Fig. 1. Scheme for role of TPPa additive on the surface of NCM811 cathode.

electronic insulator at the interface between the NCM cathode and the electrolyte. For these reasons, the electrochemical performance of TPPa was evaluated in combination with a Ni-rich NCM cathode material ($LiNi_{0.8}Co_{0.1}Mn_{0.1}O_2$, NCM811) operating at high temperature. The working mechanism of TPPa was also explored by spectroscopic analyses.

2. Experimental

The linear sweep voltammetry (LSV) measurements were conducted on a three-electrode cell assembled using Li foil (as both counter and reference electrodes) and SUS (as working electrode). The LSV was examined at a scan rate of 1 mV s^{-1} within an open circuit potential of 5.0 V (vs. Li/Li^+). The standard electrolyte consisted of ethylene carbonate (EC) and ethyl methyl carbonate (EMC) (1:2 volume ratio) containing 1 *M* lithium hexafluorophosphate ($LiPF_6$) (PanaxEtec). The TPPa-based electrolyte was composed of standard electrolyte with 2.0 wt% of TPPa (Aldrich). The TPPa was used as received without further purification.

The electrochemical performance of the cell was evaluated using a NCM811 cathode prepared as follows: 1.8 g of NCM811, 0.1 g of poly(vinylidene fluoride) (PVDF), and 0.1 g of carbon (Super P) were finely dispersed with a homogenizer in 1.5 mL of *N*-methyl pyrrolidone (NMP). The well-dispersed slurries were then cast on an Al current collector and dried in a 120°C oven for 12 h, followed by further drying in a vacuum oven at 120°C for 12 h. The electrode density of the NCM811 cathode was approxi-

mately 8.56 ± 0.73 mg cm^{-2}. The NCM811 cathode, Li foil anode, poly(ethylene) separator, and each electrolyte were then used to assemble 2032 half-cells. After cell assembly, the cells were aged for 24 h and charged/discharged from 3.0 to 4.3 V (vs. Li/Li^+) for two cycles with a 0.1 C rate (1.0 C = 200 mA g^{-1}) at 25°C as a formation step and the cells were charged/discharged with 1.0 C rate at 55°C for 100 cycles (cycle step).

Upon completion of cycling, the cells were disassembled in an Ar-filled glove box, and each NCM811 cathode was recovered. The cycled NCM811 cathode was quickly washed with dimethyl carbonate within 5 s. The surface morphology of the cycled NCM811 cathodes was analyzed by scanning electron microscopy (FE-SEM/EDS-7800F, JEOL), and the chemical composition was determined by X-ray photoelectron spectroscopy (XPS, Thermo-Scientific). The dissolved transition metal components were quantified by inductively coupled plasma mass spectrometry (ICP-MS, Bruker).

3. Results and Discussion

The electrochemical behaviors of the electrolyte were measured by LSV, as shown in Fig. 2b. No electrochemical oxidation was observed in the standard electrolyte up to 5.0 V (vs. Li/Li^+), indicating that EC and EMC do not form a CEI layer under a normal charging potential. Otherwise, the TPPa-containing electrolyte exhibited an oxidation peak at around 4.83 V (vs. Li/Li^+), implying decomposition of the TPPa by an electrochemical oxidation reaction in the cell, as would be necessary for formation of a CEI layer on the surface of cathode [59,60]. This means that TPPa may form a CEI layer on the surface of NCM811 cathode via electrochemical oxidation, as expected.

The electrochemical performances of standard and TPPa-containing electrolytes were evaluated and the results are shown in Fig. 3. At room temperature, the potential profiles of the cells were almost identical, whereas the initial specific capacity was lower in the TPPa-containing electrolyte than in the cycled standard electrolyte (Fig. 3a). This might be attributed to the relatively low ionic conductivity of the TPPa-containing electrolyte, as the standard electrolyte showed an ionic conductivity of 8.92 mS cm^{-1}, whereas the TPPa-containing electrolyte exhibited an ionic conductivity of 8.78 mS cm^{-1} as the TPPa content increased in the electrolyte.

Nonetheless, the cycling performance of the cells at room temperature did not differ appreciably (Fig. 3b). However, at the high temperature cycling, a meaningful difference was observed between the cells (Figs. 3c and 3d). The TPPa-containing electrolyte exhibited a slightly polarized potential profile with a low specific capacity (210.5 mA h g^{-1}) at the initial cycle because of its low ionic conductivity, but it showed clearly improved cycling retention after 100 cycles (retention ratio of 63.5%, 133.7 mA h g^{-1}). Conversely, the cell cycled with the standard electrolyte showed much faster fading of the cell, with a specific capacity of 108.3 mA h g^{-1} (a retention ratio of

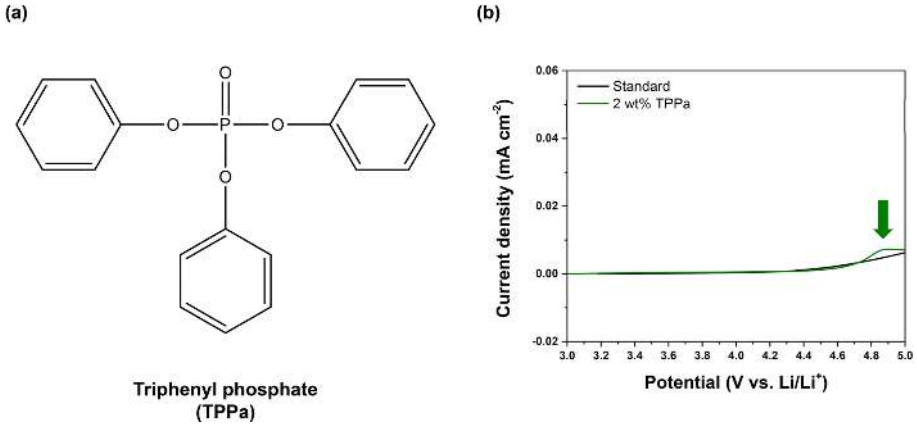

Fig. 2. (a) Molecular structure of TPPa additive, (b) LSV results for standard electrolyte (black) and TPPa-controlled electrolyte (green).

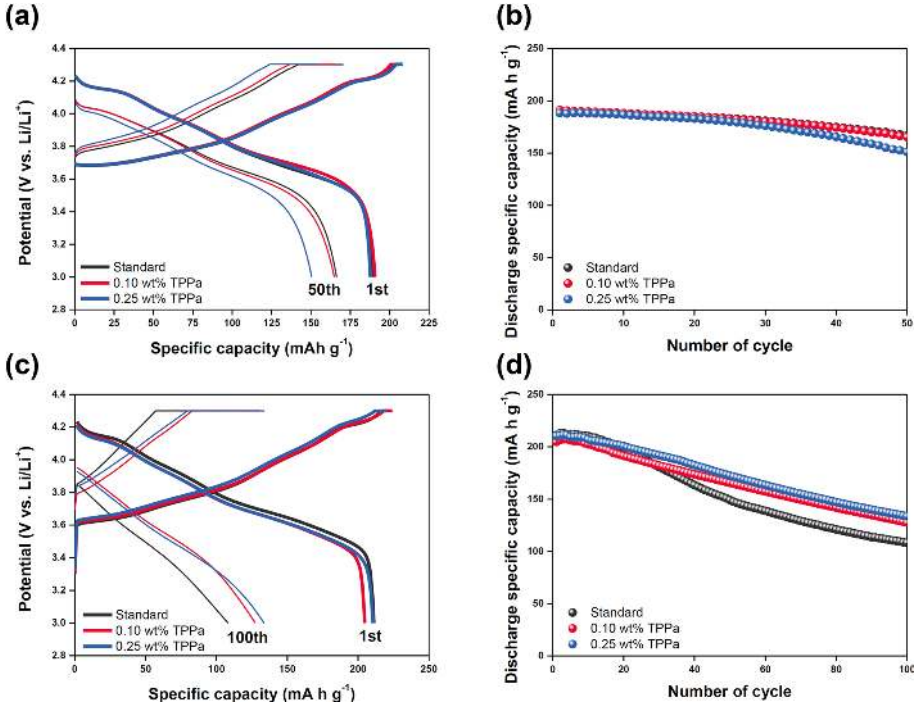

Fig. 3. (a) Potential profiles of the cells at the initial state (thick line) and after 50 cycles (thin line) and (b) Cycling behaviors of the cells at room temperature. (c) Potential profiles of the cells at the initial state (thick line) and after 100 cycles (thin line) and (d) Cycling behaviors of the cells at high temperature. (black: standard electrolyte, red: 0.10 wt%-TPPa contained electrolyte, blue: 0.25 wt%-TPPa contained electrolyte).

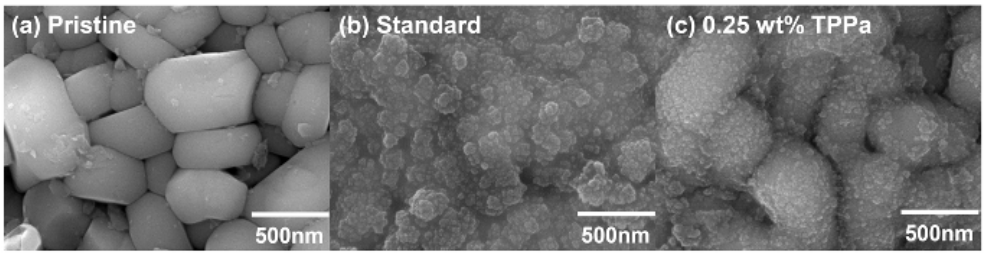

Fig. 4. Surface morphologies of (a) non-cycled NCM811, (b) cycled NCM811, and (c) cycled NCM811 with 0.25 wt% TPPa-contained electrolyte.

51.3%) at the end of cycling. Note that the electrolyte seriously decomposes at high temperatures, indicating that the addition of TPPa to the electrolyte seems effective for suppressing electrolyte decomposition because of the formation of an effective CEI layer on the surface of the NCM811 cathode.

The role of TPPa in the cell was evaluated by recovering the cycled NCM811 cathodes and analyzing their surface morphologies by SEM (Fig. 4). The surface of the recovered NCM811 cathode cycled with standard electrolyte was heavily covered with decomposed electrolyte adducts, indicating the occurrence of undesired reactions, including electrolyte decomposition, during electrochemical cycling. This observation agreed well with the electrochemical results, as once the electrolyte had decomposed on the surface of the NCM811 cathode, it hindered Li^+ migration at the interface between the NCM811 cathode and the electrolyte, resulting in fading of the cell. By contrast, cycling of the NCM811 cathode

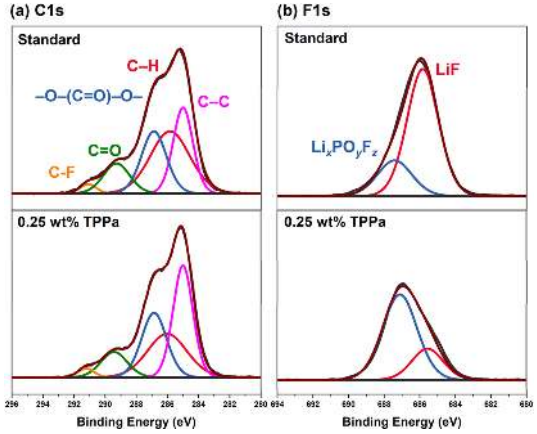

Fig. 5. XPS analyses of cycled NCM811 cathodes with standard electrolyte (up) and TPPa-controlled electrolyte (down) ((a) C1s, (b) F1s).

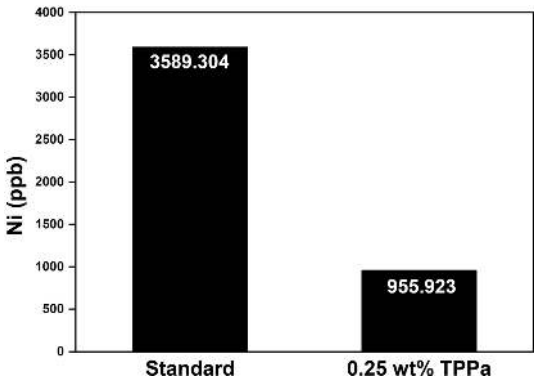

Fig. 6. ICP-MS results for cycled anodes with standard electrolyte and TPPa-contained electrolyte.

with TPPa-containing electrolyte maintained a relatively clean cathode surface state. The boundary between the primary particles of NCM811 was clearly observed and less electrolyte decomposition was noted.

These findings indicate that TPPa forms an effective CEI layer on the surface of the NCM811 cathode and is responsible for stabilizing the surface reactivity of NCM811 cathode. This possibility is also supported by the XPS analyses of the cycled NCM811 cathodes (Fig. 5). The NCM811 cathode cycled with a standard electrolyte showed a relatively low intensity of –C–F (from PVDF binder, 291.1 eV) and –C–C– (from carbon conducting agent, 285.0 eV) peaks when compared with the cathode cycled with the TPPa-containing electrolyte in the C 1s spectra, which indicate electrolyte decomposition, was significantly suppressed in the TPPa-controlled cell [61,62]. The F 1s spectra also indicated suppression of the formation of LiF (685.5 eV) in the cell cycled with TPPa-containing electrolyte. Note that LiF formation is considered evidence of electrolyte decomposition in the cell [63,64]; therefore, the TPPa additive improves the surface stability as a result of the CEI layer formation on the surface of the NCM811 cathode.

Interestingly, the cell cycled with TPPa-containing electrolyte revealed a relatively high peak intensity corresponding to $Li_xPO_yF_z$ (687.0 eV), which is considered an effective chemical composition for a CEI layer that would effectively suppress electrolyte decomposition in the cell [65-67]. Additional ICP-MS analyses of the cycled anode indicate that TPPa markedly increases the surface stability of the NCM811 cathode (Fig. 6). When compared with the cycled anode using standard electrolyte, the amount of dissolved Ni was decreased to about one quarter (3589.3 ppb vs. 955.9 ppb), which implies that the formation of the F^- component is controlled in the cell cycled with TPPa additive because the TPPa-based CEI layer effectively reduces electrolyte decomposition during the electrochemical charging/discharging processes.

4. Conclusion

Inclusion of a functional additive, TPPa, was proposed to improve the electrochemical performance of NCM811 cathode material. LSV data confirmed that TPPa was electrochemically oxidized at around 4.83 V (vs. Li/Li^+) and that TPPa participated in the formation of a CEI layer on the surface of NCM811 cathode material. At room temperature, TPPa did not compromise the cycling performance of the cell, as the cell cycled with TPPa-containing electrolyte showed a retention of 86.5% (165.4 mA h g^{-1}). At high temperature, TPPa greatly advanced the cycling performance of the NCM811 cathode material, as the cell cycled with TPPa-containing electrolyte exhibited a retention of 63.5% (133.7 mA h g^{-1}), whereas the cell cycled with standard electrolyte still suffered from poor cycling retention (51.3%, 108.3 mA h g^{-1}). Further systematic analyses of the recovered NCM811 cathodes demonstrated the effectiveness of

the TPPa-based CEI layer in the cell, as electrolyte decomposition was clearly suppressed in the cell cycled with the TPPa-containing electrolyte. The use of the TPPa-containing electrolyte also increased the surface stability of the anode, as the TPPa-based CEI layer prevented the formation of fluoride species in the cell by inhibiting electrolyte decomposition. These findings indicate that the use of TPPa is effective for increasing the surface stability of NCM811 cathode material because the TPPa-initiated PO_x-based CEI layer prevents electrolyte decomposition in the cell, even at high temperature.

Acknowledgement

This work was supported by Incheon National University Research Grant in 2019.

References

[1] J.W. Fergus, *J. Power Sources*, **2010**, *195(4)*, 939-954.
[2] B. Scrosati, J. Hassoun and Y.-K. Sun, *Energy Environ. Sci*, **2011**, *4(9)*, 3287-3295.
[3] Y.-X. Yin, S. Xin, Y.-G. Guo and L.-J. Wan, *Angew. Chem. Int. Ed.*, **2013**, *52(50)*, 13186-13200.
[4] X. Yu, Y. Lyu, L. Gu, H. Wu, S.-M. Bak, Y. Zhou, K. Amine, S.N. Ehrlich, H. Li, K.-W. Nam and X.-Q. Yang, *Adv. Energy Mater.*, **2014**, *4(5)*, 1300950.
[5] S. Zeng, L. Li, L. Xie, D. Zhao, N. Wang and S. Chen, *ChemSusChem*, **2017**, *10(17)*, 3378-3386.
[6] Y.-K. Sun, S.-T. Myung, B.-C. Park, J. Prakash, I. Belharouak and K. Amine, *Nat. Mater.*, **2009**, *8(4)*, 320-324.
[7] J.H. Lee, C.S. Yoon, J.-Y. Hwang, S.-J. Kim, F. Maglia, P. Lamp, S.-T. Myung and Y.-K. Sun, *Energy Environ. Sci*, **2016**, *9(6)*, 2152-2158.
[8] S.-T. Myung, F. Maglia, K.-J. Park, C.S. Yoon, P. Lamp, S.-J. Kim and Y.-K. Sun, *ACS Energy Lett.*, **2017**, *2(1)*, 196-223.
[9] D. Zeng, J. Cabana, J. Bréger, W.-S. Yoon and C.P. Grey, *Chem. Mater.*, **2007**, *19(25)*, 6277-6289.
[10] H.-J. Noh, S. Youn, C.S. Yoon and Y.-K. Sun, *J. Power Sources*, **2013**, *233*, 121-130.
[11] S. Hwang, S.M. Kim, S.-M. Bak, K.Y. Chung and W. Chang, *Chem. Mater.*, **2015**, *27(17)*, 6044-6052.
[12] C. Liang, F. Kong, R.C. Longo, S. Kc, J.-S. Kim, S. Jeon, S. Choi and K. Cho, *J. Phys. Chem. C*, **2016**, *120(12)*, 6383-6393.
[13] Y.-K. Sun, Z. Chen, H.-J. Noh, D.-J. Lee, H.-G. Jung, Y. Ren, S. Wang, C.S. Yoon, S.-T. Myung and K. Amine, *Nat. Mater.*, **2012**, *11(11)*, 942-947.
[14] W. Cho, S.-M. Kim, J.H. Song, T. Yim, S.-G. Woo, K.-W. Lee, J.-S. Kim and Y.-J. Kim, *J. Power Sources*, **2015**, *282*, 45-50.
[15] S. Neudeck, F. Walther, T. Bergfeldt, C. Suchomski, M. Rohnke, P. Hartmann, J. Janek and T. Brezesinski, *ACS Appl. Mater. Interfaces*, **2018**, *10(24)*, 20487-20498.
[16] L. Zhang, T. Dong, X. Yu, Y. Dong, Z. Zhao and H. Li, *j.materresbull*, **2012**, *47(11)*, 3269-3272.
[17] T. Yim, K.S. Kang, J. Mun, S.H. Lim, S.-G. Woo, K.J. Kim, M.-S. Park, W. Cho, J.H. Song, Y.-K. Han, J.-S. Yu and Y.-J. Kim, *J. Power Sources*, **2016**, *302*, 431-438.
[18] K. Heo, J.-S. Lee, H.-S. Kim, J. Kim and J. Lim, *J. Electrochem. Soc.*, **2017**, *164(12)*, A2398-A2402.
[19] S. Dong, Y. Zhou, C. Hai, J. Zeng, Y. Sun, Y. Shen, X. Li, X. Ren, G. Qi, X. Zhang and L. Ma, *Ceramics International*, **2019**, *45(1)*, 144-152.
[20] J.-S. Lee, K. Heo, H.-S. Kim, M.-Y. Kim, J. Kim, S.-W. Kang and J. Lim, *J. Alloys Compd.*, **2019**, *781*, 553-559.
[21] J. Li, L.E. Downie, L. Ma, W. Qiu and J.R. Dahn, *J. Electrochem. Soc.*, **2015**, *162(7)*, A1401-A1408.
[22] M. Wang, R. Zhang, Y. Gong, Y. Su, D. Xiang, L. Chen, Y. Chen, M. Luo and M. Chu, *Solid State Ion.,* **2017**, *312*, 53-60.
[23] A. Iqbal, L. Chen, Y. Chen, Y.-x. Gao, F. Chen and D.-c. Li, *Int. J. Miner. Metall. Mater*, **2018**, *25(12)*, 1473-1481.
[24] Q. Gan, N. Qin, Y. Zhu, Z. Huang, F. Zhang, S. Gu, J. Xie, K. Zhang, L. Lu and Z. Lu, *ACS Appl. Mater. Interfaces,* **2019**, *11(13)*, 12594-12604.
[25] H.Q. Pham, E.-H. Hwang, Y.-G. Kwon and S.-W. Song, *ChemComm*, **2019**, *55(9)*, 1256-1258.
[26] L. Wu, K.-W. Nam, X. Wang, Y. Zhou, J.-C. Zheng, X.-Q. Yang and Y. Zhu, *Chem. Mater.*, **2011**, *23(17)*, 3953-3960.
[27] S. Hwang, S.M. Kim, S.-M. Bak, B.-W. Cho, K.Y. Chung, J.Y. Lee, W. Chang and E.A. Stach, *ACS Appl. Mater. Interfaces*, **2014**, *6(17)*, 15140-15147.
[28] H.-R. Kim, S.-G. Woo, J.-H. Kim, W. Cho and Y.-J. Kim, *J. Electroanal. Chem.*, **2016**, *782*, 168-173.
[29] L. Liang, G. Hu, F. Jiang and Y. Cao, *J. Alloys Compd.*, **2016**, *657*, 570-581.
[30] F. Schipper, E.M. Erickson, C. Erk, J.-Y. Shin, F.F. Chesneau and D. Aurbach, *J. Electrochem. Soc.*, **2017**, *164(1)*, A6220-A6228.
[31] J. Cho, Y.J. Kim, T.-J. Kim and B. Park, *Angew. Chem. Int. Ed.*, **2001**, *40(18)*, 3367-3369.
[32] D. Li, Y. Kato, K. Kobayakawa, H. Noguchi and Y. Sato, *J. Power Sources*, **2006**, *160(2)*, 1342-1348.
[33] S. Neudeck, F. Strauss, G. Garcia, H. Wolf, J. Janek, P. Hartmann and T. Brezesinski, *ChemComm*, **2019**, *55(15)*, 2174-2177.
[34] H. Zhang, J. Xu and J. Zhang, *Front. Mater.*, **2019**, *6(309),*1-10.
[35] V.-C. Ho, S. Jeong, T. Yim and J. Mun, *J. Power Sources*, **2020**, *450*, 227625.
[36] X. Lu, X. Li, Z. Wang, H. Guo, G. Yan and X. Yin, *Appl. Surf. Sci.*, **2014**, *297*, 182-187.
[37] H. Kim, M.G. Kim, H.Y. Jeong, H. Nam and J. Cho,

Nano Lett., **2015**, *15(3)*, 2111-2119.
[38] B.-J. Chae and T. Yim, *J. Power Sources*, **2017**, *360*, 480-487.
[39] B.-J. Chae, J.H. Park, H.J. Song, S.H. Jang, K. Jung, Y.D. Park and T. Yim, *Electrochim. Acta*, **2018**, *290*, 465-473.
[40] H.J. Song, S.H. Jang, J. Ahn, S.H. Oh and T. Yim, *J. Power Sources*, **2019**, *416*, 1-8.
[41] Y.-K. Han, J. Yoo and T. Yim, *Electrochim. Acta*, **2016**, *215*, 455-465.
[42] K. Kim, Y. Kim, S. Park, H.J. Yang, S.J. Park, K. Shin, J.-J. Woo, S. Kim, S.Y. Hong and N.-S. Choi, *J. Power Sources*, **2018**, *396*, 276-287.
[43] B. Zhang, N. Laszczynski and B.L. Lucht, *Electrochim. Acta*, **2018**, *281*, 405-409.
[44] Y. Lin, X. Yue, H. Zhang, L. Yu, W. Fan and T. Xie, *Electrochim. Acta*, **2019**, *300*, 202-207.
[45] S. Wang, S. Chen, W. Gao, L. Liu and S. Zhang, *J. Power Sources*, **2019**, *423*, 90-97.
[46] K. Beltrop, S. Klein, R. Nölle, A. Wilken, J.J. Lee, T.K.J. Köster, J. Reiter, L. Tao, C. Liang, M. Winter, X. Qi and T. Placke, *Chem. Mater.*, **2018**, *30(8)*, 2726-2741.
[47] S.H. Jang, K. Jung and T. Yim, *Curr. Appl. Phys.,* **2018,** *18(11)*, 1345-1351.
[48] C.-G. Shi, C.-H. Shen, X.-X. Peng, C.-X. Luo, L.-F. Shen, W.-J. Sheng, J.-J. Fan, Q. Wang, S.-J. Zhang, B.-B. Xu, J.-J. Xian, Y.-M. Wei, L. Huang, J.-T. Li and S.-G. Sun, *Nat. Energy,* **2019**, *65*, 104084.
[49] S. Li, T. Yang, W. Wang, J. Lu, X. Zhao, W. Fan, X. Zuo and J. Nan, *Electrochim. Acta*, **2020**, *352*, 136492.
[50] L. Liu, W. Gao, Y. Cui and S. Chen, *J. Alloys Compd.*, **2020**, *820*, 153069.
[51] Y.-M. Song, J.-G. Han, S. Park, K.T. Lee and N.-S. Choi, *J. Mater. Chem. A*, **2014**, *2(25)*, 9506-9513.
[52] Z. Zhou, Y. Ma, L. Wang, P. Zuo, X. Cheng, C. Du, G. Yin and Y. Gao, *Electrochim. Acta*, **2016**, *216*, 44-50.
[53] C. Peebles, R. Sahore, J.A. Gilbert, J.C. Garcia, A. Tornheim, J. Bareño, H. Iddir, C. Liao and D.P. Abraham, *J. Electrochem. Soc.*, **2017**, *164(7)*, A1579-A1586.
[54] N. von Aspern, S. Röser, B. Rezaei Rad, P. Murmann, B. Streipert, X. Mönnighoff, S.D. Tillmann, M. Shevchuk, O. Stubbmann-Kazakova, G.-V. Röschenthaler, S. Nowak, M. Winter and I. Cekic-Laskovic, *J. Fluorine Chem.*, **2017**, *198*, 24-33.
[55] L. Wang, Y. Ma, Q. Li, Y. Cui, P. Wang, X. Cheng, P. Zuo, C. Du, Y. Gao and G. Yin, *Electrochim. Acta*, **2017**, *243*, 72-81.
[56] S. Tan, Z. Zhang, Y. Li, Y. Li, J. Zheng, Z. Zhou and Y. Yang, *J. Electrochem. Soc.*, **2013**, *160(2)*, A285-A292.
[57] S. Mai, M. Xu, X. Liao, J. Hu, H. Lin, L. Xing, Y. Liao, X. Li and W. Li, *Electrochim. Acta*, **2014**, *147*, 565-571.
[58] S. Mai, M. Xu, X. Liao, L. Xing and W. Li, *J. Power Sources*, **2015**, *273*, 816-822.
[59] K. Abe, Y. Ushigoe, H. Yoshitake and M. Yoshio, *J. Power Sources*, **2006**, *153(2)*, 328-335.
[60] X. Zuo, C. Fan, J. Liu, X. Xiao, J. Wu and J. Nan, *J. Power Sources*, **2013**, *229*, 308-312.
[61] D. Aurbach, Y Ein?Ely and A Zaban, *J. Electrochem. Soc.*, **1994**, *141(1)*, L1-L3.
[62] S.J. An, J. Li, C. Daniel, D. Mohanty, S. Nagpure and D.L. Wood, *Carbon*, **2016**, *105*, 52-76.
[63] D. Ensling, M. Stjerndahl, A. Nytén, T. Gustafsson and J.O. Thomas, *J. Mater. Chem.*, **2009**, *19(1)*, 82-88.
[64] M. Xu, W. Li and B.L. Lucht, *J. Power Sources*, **2009**, *193(2)*, 804-809.
[65] J.-G. Han, I. Park, J. Cha, S. Park, S. Park, S. Myeong, W. Cho, S.-S. Kim, S.Y. Hong, J. Cho and N.-S. Choi, *ChemElectroChem*, **2017**, *4(1)*, 56-65.
[66] T. Yim and Y.-K. Han, *ACS Appl. Mater. Interfaces*, **2017**, *9(38)*, 32851-32858.
[67] Y. Lin, H. Zhang, X. Yue, L. Yu and W. Fan, *J. Electroanal. Chem.*, **2019**, *832*, 408-416.